



**HAL**  
open science

## Functionalization of chitosan with lignin to produce active materials by waste valorization

Kevin Crouvisier-Urien, Fernanda Regina da Silva Farias, Sorawit Arunatat, Donnchadh Griffin, Massimiliano Gerometta, Jeancarlo Rocca-Smith, Guy Weber, Nicolas Sok, Thomas Karbowiak

### ► To cite this version:

Kevin Crouvisier-Urien, Fernanda Regina da Silva Farias, Sorawit Arunatat, Donnchadh Griffin, Massimiliano Gerometta, et al.. Functionalization of chitosan with lignin to produce active materials by waste valorization. *Green Chemistry*, 2019, 21 (17), pp.4633-4641. 10.1039/c9gc01372e . hal-02372038

**HAL Id: hal-02372038**

**<https://hal.science/hal-02372038>**

Submitted on 25 Nov 2020

**HAL** is a multi-disciplinary open access archive for the deposit and dissemination of scientific research documents, whether they are published or not. The documents may come from teaching and research institutions in France or abroad, or from public or private research centers.

L'archive ouverte pluridisciplinaire **HAL**, est destinée au dépôt et à la diffusion de documents scientifiques de niveau recherche, publiés ou non, émanant des établissements d'enseignement et de recherche français ou étrangers, des laboratoires publics ou privés.

## Functionalization of chitosan with lignin to produce active materials by waste valorization

Received 00th January 20xx,  
Accepted 00th January 20xx

DOI: 10.1039/x0xx00000x

www.rsc.org/

Kevin Crouvisier Urion,<sup>a</sup> Fernanda Da Silva Farias,<sup>a</sup> Sorawit Arunatat,<sup>a</sup> Donnchadh Griffin,<sup>a</sup> Massimiliano Gerometta,<sup>a</sup> Jean-Carlo Rocca Smith,<sup>a</sup> Guy Weber,<sup>b</sup> Nicolas Sok,<sup>a</sup> and Thomas Karbowskiak<sup>\*a</sup>

The valorization of lignin to produce functionalized materials is challenging. A grafting reaction based on the reactivity between chitosan amino groups and lignin hydroxyl groups was performed, in an environmentally friendly solvent to produce thin films that can be used as active packaging or coating materials. A systematic comprehensive study was performed, that focused first on the grafting of the three phenolic acids composing lignin (coumaric, ferulic, and sinapic acids), and then of the lignin polymer itself on chitosan. The anti-oxidant activity of lignin monomers was preserved after grafting onto chitosan with significant differences regarding their initial radical scavenging activity: sinapic acid > ferulic acid > coumaric acid. The lignin polymer can also be grafted onto chitosan, which results in an intermediate anti-oxidant activity of the film. Therefore, this work opens a new route for the valorization of lignin, with the possibility of tuning the anti-oxidant activity of the final material based on the appropriate selection of the initial sustainable resource.

### Introduction

Lignin is an abundant natural amorphous polymer and a cheap by-product of paper production, cellulosic industries and ethanol bio-refineries,<sup>1-4</sup> which annually produce millions of tons of this polymer.<sup>5</sup> Lignin is the second most abundant component in wood after cellulose (18-35 %wt of the dry matter).<sup>6</sup> Not only is it one of the main components of wood, but also of fruits and vegetables, representing 20 %wt of the worldwide biomass.<sup>7</sup> It is difficult to characterize the exact chemical composition of lignin because of the extraction process from the biomass, into which non-native chemical species can be introduced.<sup>8</sup> Nevertheless, a general empirical molecular formula for the lignin monomer can be determined as  $C_9H_{(10-n)}O_2(OCH_3)_n$ , with  $n$  being the mean ratio of the methoxy groups on the aromatic rings of the lignin monomer (Figure 1). Based on the value of  $n$ , the three phenyl propene lignin monomers can be divided into the following units: the *p*-hydroxyphenyl unit ( $n = 0$ ; H unit), the guaiacyl unit ( $n = 1$ ; G unit) and the syringyl unit ( $n = 2$ ; S unit).<sup>4,9</sup> These units are commonly referred to as coumaric, ferulic, and sinapic acids when present as free monomers, respectively. The macromolecular structure of lignin depends on the ratio and random polymerization of the monomers, according to their

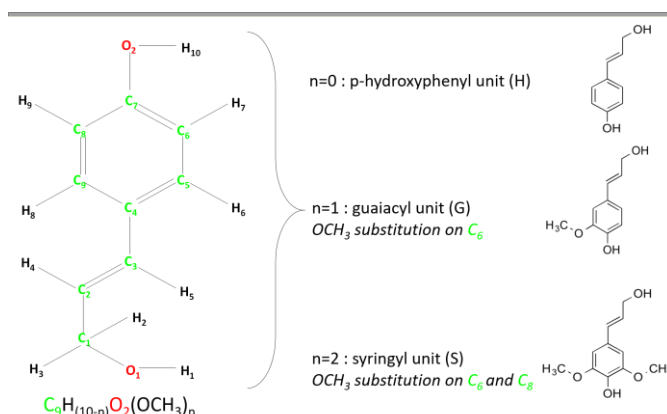


Figure 1: General condensed formula of lignin monomer, with detailed chemical structure of the three monolignols corresponding to the degree of methyl-substitution on the aromatic ring. The global value of  $n$  depends on the respective proportion of these three sub-units in the lignin: H (*p*-hydroxyphenyl), G (guaiacyl) and S (syringyl).

botanical origin.<sup>10,11</sup> The resulting lignin is an important structural polymer in the plant cell wall, providing antimicrobial resistance, low permeability, and high mechanical resistance.<sup>9,12</sup> Another interesting property of lignin is its anti-oxidant activity due to the hydroxyl groups on the aromatic ring (Ar-OH, MeO-Ar-OH, (MeO)<sub>2</sub>-Ar-OH).<sup>13</sup> Currently, lignin is mostly used as a low-cost fuel. However, recent studies described the use of this by-product as a value-adding commodity in polymer production. One of the strategies adopted for lignin valorization is the incorporation into polymer matrices,<sup>14,15</sup> using blending,<sup>16</sup> solvent casting,<sup>13,17,18</sup> layer-by-layer<sup>19,20</sup> or spin coating.<sup>21</sup> These

<sup>a</sup> Univ. Bourgogne Franche-Comté, Agrosup Dijon, PAM UMR A 02.102, F-21000, Dijon, France

<sup>b</sup> Univ. Bourgogne Franche-Comté, Laboratoire Interdisciplinaire Carnot de Bourgogne, UMR 6303 CNRS, 9 Avenue Alain Savary, F-21078, Dijon, France  
\*Email : thomas.karbowskiak@agrosupdijon.fr

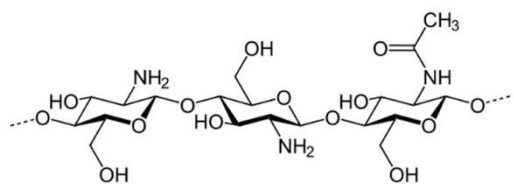


Figure 2: Structure of the chitosan polymer (at pH > pKa amino group) displaying both acetylated and deacetylated monomer units.

methods have already been applied in the production of conventional polymers, such as polypropylenes (flame retardants),<sup>3</sup> polystyrenes (filler applications),<sup>10</sup> or carbon fibres and polyacrylamides (material reinforcements).<sup>22,23</sup> Furthermore, more sustainable matrices such as starch,<sup>24</sup> soy protein,<sup>25</sup> and chitosan<sup>13,17,18</sup> can also be used for application as films. Indeed, chitosan is a potential candidate for the replacement of conventional plastics due to its film-forming capacity (giving transparent and resistant films) and high oxygen barrier property.<sup>13,26,27</sup> This is also a waste product from the marine industry that can be valorized. Its structure, derived from chitin deacetylation, is shown in Figure 2. The incorporation of lignin is targeted to confer antioxidant activity<sup>13</sup> or UV-barrier property<sup>28</sup> to packaging materials in order to protect sensitive products, such as foods or cosmetics, against oxidation. However, chitosan and lignin are non-thermodynamically compatible polymers since chitosan is hydrophilic and soluble in aqueous phase, while lignin is hydrophobic and soluble in organic phase. Because of this poor compatibility, the physical incorporation of lignin into chitosan matrix leads to a heterogeneous system in which lignin aggregates are distributed within the polymer network.<sup>13,17</sup> This even occurs at a very low lignin percentage (> 2.5 %wt).<sup>13</sup> Physical treatment, such as high pressure processing, can improve the lignin dispersion but also induces migration of lignin residues.<sup>18</sup>

The objective of this study was to investigate the use of using chemical grafting to improve the compatibility of chitosan and lignin and to assess whether grafting preserves anti-oxidant activity. In the present work, grafting was carried out with lignin, but also with the different lignin monomers, in order to identify the origin of lignin's anti-oxidant activity and the effect of grafting using a systematic comprehensive approach.

## Experimental

### Material

Chitosan with a deacetylation degree of 90 %, was supplied by France Chitin (France). Its weight-average molecular weight  $\overline{M}_w$  was 274 kDa ( $\pm 32$ ), and its number-average molecular weight  $\overline{M}_n$  was 163 kDa ( $\pm 9$ ).<sup>29</sup> Lignin used for this study, provided by Granit SA (Swiss), was extracted from sugar cane (*Saccharum munja*) by an alkaline process. This type of lignin is usually referred to as "Sarkanda". It has a G/S unit ratio of 1.04 and a low content of free phenolic monomers with around 0.5 mg.g<sup>-1</sup>.

The three acid phenols corresponding to the three lignin monomers (Figure 1) used in this study were coumaric acid (98 % purity), trans-ferulic acid (99 % purity) and sinapic acid (98 % purity). Acetic acid (99 % purity), ethanol (99.8 % purity), N-hydroxysuccinimide (NHS; 98 % purity) and N-(3-dimethylaminopropyl)-N'-ethylcarbodiimide hydrochloride (EDC; 98 % purity) were purchased from Merck (Germany).

### Grafting of lignin monomers and lignin polymer onto chitosan

The synthesis reaction was adapted from the protocol described by Woranuch *et al.* (2013),<sup>30</sup> and a molar ratio of chitosan monomer to lignin monomer close to one was used. First, a chitosan solution (1.2 % w/v) was prepared by dispersing 0.6 g of chitosan in an aqueous solution composed of 0.5 mL of acetic acid and 49.5 mL of distilled water at 25 °C for 12 h. To obtain an activated ester of each lignin monomer, 0.648 g of ferulic acid, 0.548 g of coumaric acid, or 0.748 g of sinapic acid, were mixed with NHS (0.384 g) and EDC (0.518 g) in 10 mL of ethanol for 30 min. The same protocol was used to obtain activated lignin polymer, using 0.6 g of lignin. Afterwards, this activated ester solution of lignin monomer or lignin polymer (10 mL) was added into the chitosan solution (50 mL), and the final solution was stirred for 12 h at 60 °C (pH  $\approx$  6). The mixture was then dialysed (using 3500 Da molecular weight cut off for the lignin monomers and 100 000 Da molecular weight cut off for the lignin) with distilled water as buffer. To ensure elimination of free acids and by-products of the reactions, dialysis was repeated 10 times within 5 days. Self-standing films (of around 40  $\mu$ m thickness) were obtained by casting and solvent evaporation of the dialysed solution, at 25 °C and 50 % relative humidity.

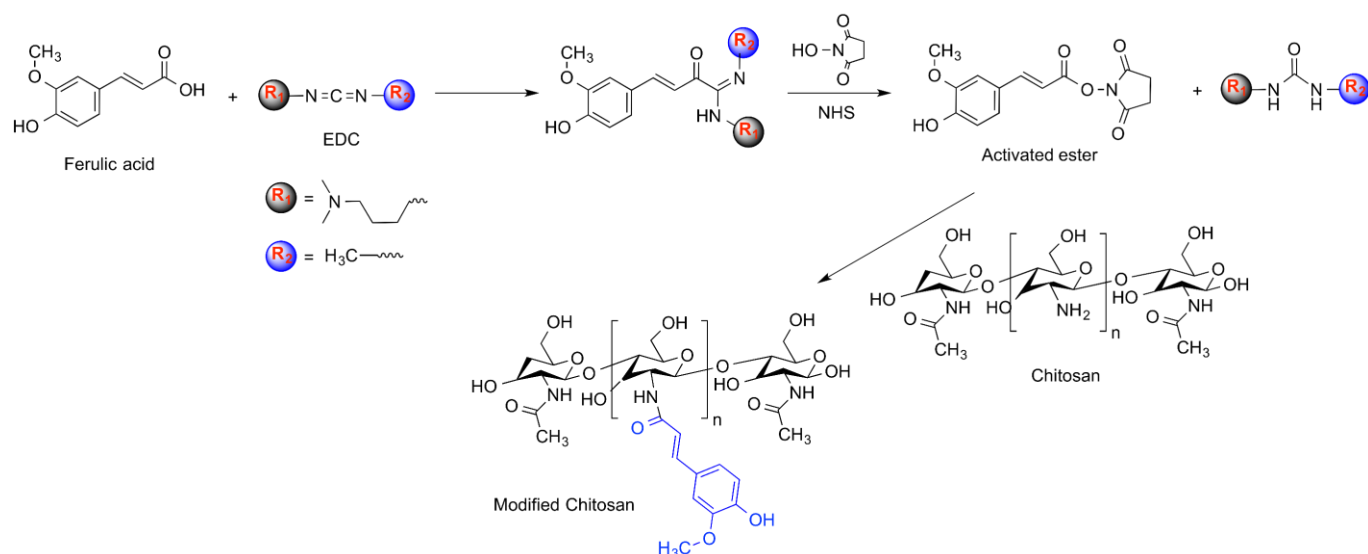
### Characterization of the grafting reaction onto chitosan

Elemental analysis was carried out using a Thermo Electron Flash EA 1112 Series CHNS/O analyser. Around 1 mg of sample was pyrolysed with excess oxygen at 960 °C, and three replicates were analysed.

UV-Vis absorbance spectra were recorded at a wavelength range of 200-800 nm (Safas mc1 UV-Vis spectrophotometer). After grafting and dialysis, the casting solution was analysed, using acetic acid solution (1 % v/v) as blank, and lignin monomer (1 % m/v) in acetic acid solution (1 % v/v) as control. Fourier Transform InfraRed (FTIR) absorbance spectra of the starting materials (lignin monomers, lignin and chitosan) and of the grafted films were recorded at 25 °C at a spectral range from 400 to 4000 cm<sup>-1</sup> using a Bruker Equinox 55 spectrophotometer equipped with a global source, DTGS detector and KBr splitter. Absorbance spectra were recorded in transmission mode with a resolution of 2 cm<sup>-1</sup> and an average of 100 scans per analysis, using a KBr pellet (200 mg) as reference. For sample preparation, KBr pellets were pressed after mixing 199 mg of KBr and 1 mg of solid material.

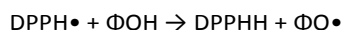
### Anti-oxidant activity

A DPPH• ( $\alpha$ -diphenyl- $\beta$ -picrylhydrazyl) test was used to measure the Radical Scavenging Activity (RSA) of films,



Scheme 1: Chemical pathway for ferulic acid grafting onto chitosan using ester activation of the lignin monomer. The coupling agents (NHS and EDC) transformed the acid function of the ferulic acid (RCOOH) into a reactive ester (RCOOR). The intermediate activated ester reacts on the amine I of the chitosan deacetylated unit, by nucleophilic substitution. Coumaric and sinapic acids, as well as lignin, were also grafted following the same reaction.

according to the method recently proposed by Crouvisier-Urien *et al.*<sup>13</sup> This method is based on the reduction of the free stable radical scavenging molecule DPPH• in the presence of a phenolic compound ( $\Phi$ -OH). DPPH• displays a purple colour ( $\lambda = 515$  nm) as a free radical and a yellow color in its reduced form (DPPHH). In the present work, this test was performed in ethanol, in which the DPPH• is soluble while the chitosan film is not soluble, thus preserving the integrity of the film during the experiment. During the reaction, free radicals are captured by the transfer of the H from  $\Phi$ -OH to DPPH•, which is then converted into the stable DPPHH molecule:<sup>31,32</sup>



First, the anti-oxidant activity of the three initial lignin monomers was determined. A monomer solution at 20 mg.L<sup>-1</sup> in ethanol was used, from which 5 mL were added to 5 mL of an ethanol DPPH• solution at 100 mg.L<sup>-1</sup>. Lignin cannot be tested with this method since there is an overlapping of the absorbance of DPPH•. For the films (with or without grafting), the samples were prepared by stirring 10 cm<sup>2</sup> of each film in 10 mL of an ethanol DPPH• solution at 50 mg.L<sup>-1</sup>. The final concentration of the DPPH• solution was thus fixed at 50 mg.L<sup>-1</sup> both for the powder and the film samples.

The kinetics of the reaction were followed at 25 °C by the disappearance of the DPPH• free radical using absorbance measurement at  $\lambda = 515$  nm with a UV-visible spectrophotometer (Biochrom WPA lightwave II). The DPPH• solution (2 mL) was sampled and returned to the original solution after each absorbance reading. Samples were maintained in closed vials covered by aluminium foil to protect them from light and stirred (200 rpm), until the reaction equilibrium was reached.

The reduction in radical scavenging activity, RSA(t), in %, was expressed as:

$$\text{RSA}(\%) = 100 - [(A_{\text{blank}}(t) - A_{\text{sample}}(t))/A_{\text{blank}}(t)] \times 100$$

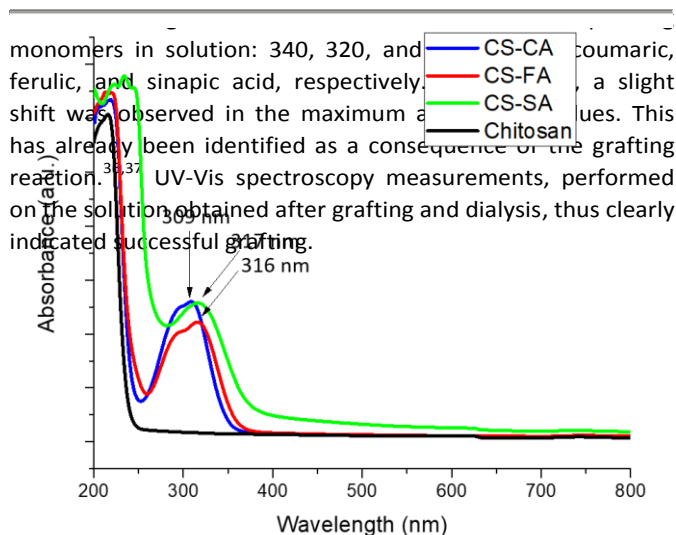
where  $A_{\text{sample}}(t)$  is the absorbance measured for the DPPH• solution containing the sample at time  $t$ , and  $A_{\text{blank}}(t)$  is the absorbance of the DPPH• solution at the same time. This correction takes into account the kinetics of DPPH• auto-degradation. Thus, RSA(t) values represent the anti-oxidant capacity of the sample. Kinetics measurements were done in triplicate, at least.

## Results and discussion

### Grafting of lignin monomers onto chitosan

Lignin monomers were grafted onto chitosan by ester activation through a carbodiimide-mediated coupling reaction in acetic acid solution (1 % v/v) with EDC and NHS, using a molar ratio of lignin/chitosan monomer close to one. By using this method, the coupling agents transformed the acid function of the ferulic acid (RCOOH) into a reactive ester (RCOOR). Amide linkage was created by nucleophilic substitution of the ferulic activated ester on the reactive primary amine function of the chitosan,<sup>30,33</sup> as shown in Scheme 1.

In order to validate the grafting reaction of the lignin monomers onto chitosan, UV-Vis spectroscopy was first performed on the solution obtained after the grafting reaction and dialysis, and just before casting (Figure 3). In the range of 250-800 nm, chitosan in solution did not exhibit any absorbance peak. However, after the grafting reaction with lignin monomers, absorbance peaks were noticed. Chitosan solutions grafted with coumaric acid, ferulic acid, and sinapic acid, displayed characteristic absorbance peaks with maxima at 309, 316, and 317 nm, respectively. These values were in



films (Figure 5), it was noteworthy that, for all three films grafted with lignin monomers, shifts occurred from  $1603\text{ cm}^{-1}$  ( $\delta_{\text{N-H}}$  of the amine I groups) down to around  $1560\text{ cm}^{-1}$  ( $\delta_{\text{N-H}}$  of the amine II groups). This was completely in accordance with the grafting reaction (Scheme 1), because the grafting took place on the amine group of the deacetylated chitosan monomer units, which therefore change the local environment of the corresponding nitrogen atom. Furthermore, the characteristic peaks of each monomer also appeared on the corresponding film spectra, especially peaks attributing to stretching vibrations of the aromatic ring (around  $1520$  and  $1462\text{ cm}^{-1}$ ),  $\nu_{\text{C-O}}$  of the hydroxyl groups for ferulic acid ( $1277\text{ cm}^{-1}$ ) and  $\beta_{\text{C-H}}$  of the aromatic ring for sinapic acid ( $1114\text{ cm}^{-1}$ ). The presence of these new absorbance peaks in the final composite polymer was thus additional evidence that lignin monomers were successfully grafted onto chitosan. Following spectroscopic analysis, that proved the successful

grafting reaction (followed by dialysis) of lignin monomers onto chitosan (CS: chitosan, CA: coumaric acid, FA: ferulic acid, SA: sinapic acid). Chitosan spectrum in solution is also displayed for comparison purpose. The arrows point out characteristic maximum absorbance peaks.

To go further in the analysis of the grafting, FTIR absorbance spectra were also determined, first on lignin monomers and

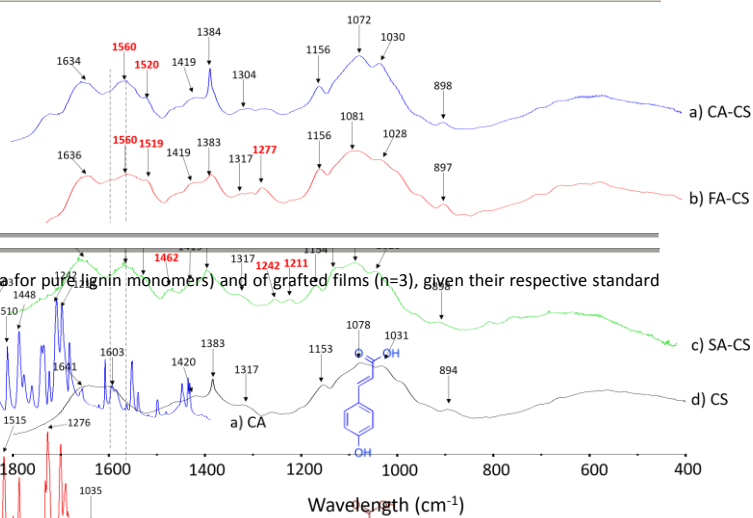


Table 1: Elemental composition of starting materials (calculated from their empirical formula) for pure lignin monomers and of grafted films (n=3), given their respective standard deviation. C/N ratio and grafted yield (expressed as molar %) are also reported.

coumaric acid groups and  $\nu_{\text{C-H}}$  of the aromatic ring),  $1673\text{ cm}^{-1}$  ( $\nu_{\text{C=O}}$  of the carboxylic acid groups and  $\nu_{\text{C=C}}$  of the aromatic ring),  $1603$ ,  $1510$ , and  $1448\text{ cm}^{-1}$  ( $\nu_{\text{C=C}}$  of the aromatic ring),  $1242\text{ cm}^{-1}$  ( $\beta_{\text{C-H}}$  of aromatic ring), and  $1214\text{ cm}^{-1}$  ( $\beta_{\text{O-H}}$  and  $\nu_{\text{C=O}}$  of the aromatic ring). Ferulic acid exhibited characteristic peaks (Figure 4b, red line) at  $3439\text{ cm}^{-1}$  ( $\nu_{\text{O-H}}$  of the hydroxyl groups),  $3077$ - $2514\text{ cm}^{-1}$  ( $\nu_{\text{O-H}}$  of the hydroxyl groups),  $1697\text{ cm}^{-1}$  ( $\nu_{\text{C=O}}$  of the carboxylic acid groups),  $1617$  and  $1518\text{ cm}^{-1}$  ( $\nu_{\text{C=C}}$  of the aromatic ring),  $1461\text{ cm}^{-1}$  ( $\nu_{\text{C=C}}$  of the aromatic ring and  $\beta_{\text{O-CH}_3}$ ),  $1368\text{ cm}^{-1}$  ( $\nu_{\text{C=C}}$  of the aromatic ring),  $1247\text{ cm}^{-1}$  ( $\nu_{\text{C-O}}$ ),  $1209\text{ cm}^{-1}$  ( $\nu_{\text{C-O}}$  and  $\beta_{\text{O-H}}$ ), and  $1115\text{ cm}^{-1}$  ( $\beta_{\text{C-H}}$  of the aromatic ring). Sinapic acid displayed main characteristic peaks (Figure 4c, green line) at  $3372$  and  $3245\text{ cm}^{-1}$  ( $\nu_{\text{O-H}}$  of the hydroxyl groups),  $3081$ - $2846\text{ cm}^{-1}$  ( $\nu_{\text{O-H}}$  of the carboxylic acid groups and  $\nu_{\text{C-H}}$  of the aromatic ring),  $1697\text{ cm}^{-1}$  ( $\nu_{\text{C=O}}$  of the carboxylic acid groups),  $1617$  and  $1518\text{ cm}^{-1}$  ( $\nu_{\text{C=C}}$  of the aromatic ring),  $1461\text{ cm}^{-1}$  ( $\nu_{\text{C=C}}$  of the aromatic ring and  $\beta_{\text{O-CH}_3}$ ),  $1368\text{ cm}^{-1}$  ( $\nu_{\text{C=C}}$  of the aromatic ring),  $1247\text{ cm}^{-1}$  ( $\nu_{\text{C-O}}$ ),  $1209\text{ cm}^{-1}$  ( $\nu_{\text{C-O}}$  and  $\beta_{\text{O-H}}$ ), and  $1115\text{ cm}^{-1}$  ( $\beta_{\text{C-H}}$  of the aromatic ring). Chitosan spectrum displayed characteristic peaks (Figure 4d, black line) at  $3439\text{ cm}^{-1}$  ( $\nu_{\text{O-H}}$  of the hydroxyl groups),  $3077$ - $2514\text{ cm}^{-1}$  ( $\nu_{\text{O-H}}$  of the hydroxyl groups),  $1697\text{ cm}^{-1}$  ( $\nu_{\text{C=O}}$  of the carboxylic acid groups),  $1617$  and  $1518\text{ cm}^{-1}$  ( $\nu_{\text{C=C}}$  of the aromatic ring),  $1461\text{ cm}^{-1}$  ( $\nu_{\text{C=C}}$  of the aromatic ring and  $\beta_{\text{O-CH}_3}$ ),  $1368\text{ cm}^{-1}$  ( $\nu_{\text{C=C}}$  of the aromatic ring),  $1247\text{ cm}^{-1}$  ( $\nu_{\text{C-O}}$ ),  $1209\text{ cm}^{-1}$  ( $\nu_{\text{C-O}}$  and  $\beta_{\text{O-H}}$ ), and  $1115\text{ cm}^{-1}$  ( $\beta_{\text{C-H}}$  of the aromatic ring).

Figure 5: FTIR absorbance spectra obtained on grafted films with a) coumaric acid (CS-CA); b) ferulic acid (CS-FA), c) sinapic acid (CS-SA) and d) initial chitosan (CS) spectrum for comparison purpose. Spectra were only considered in the  $1800$ - $400\text{ cm}^{-1}$  range to better highlight differences. The arrows represent the characteristic maximum absorbance peaks. Vibrations in red refer to the differences noticed between initial chitosan film and chitosan grafted films. The dashed lines indicate the shift occurring from  $1603\text{ cm}^{-1}$  ( $\delta_{\text{N-H}}$  of the amine I group) down to around  $1560\text{ cm}^{-1}$  ( $\delta_{\text{N-H}}$  of the amine II group) after the grafting.

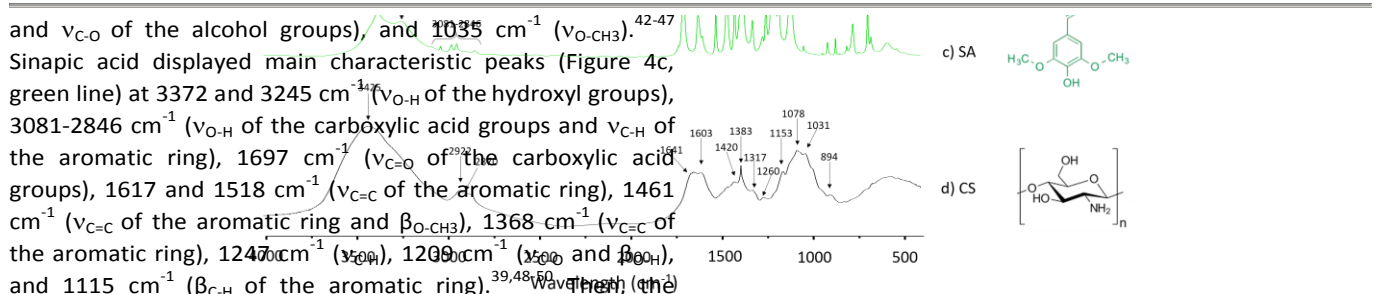


Figure 4: FTIR absorbance spectra of starting materials: a) coumaric acid (CA); b) ferulic acid (FA), c) sinapic acid (SA) and d) chitosan (CS). The arrows represent the characteristic maximum absorbance peaks.

Sample	Nitrogen ( $\delta_{\text{N-H}}$ of the amine I group), $1420\text{ cm}^{-1}$ ( $\delta_{\text{CH}_2}$ )	Carbon ( $\delta_{\text{C-H}}$ of the primary hydroxyl groups), $1383\text{ cm}^{-1}$ ( $\delta_{\text{OH}}$ )	Hydrogen (wt %)	Sulfur (wt %)	C/N Ratio	Grafted yield (%)
Chitosan (90% deacetylated)	-	-	$6.58 \pm 0.33$	0	$5.52 \pm 0.15$	-
coumaric acid (CA)	-	-	4.87	0	0	-
CS-CA film	$5.59 \pm 0.24$	$39.85 \pm 0.24$	$6.17 \pm 0.13$	0	$6.93 \pm 0.27$	$13.8 \pm 3.3$
ferulic acid (FA)	-	-	5.12	0	0	-
CS-FA film	$5.59 \pm 0.24$	$39.85 \pm 0.24$	$6.12 \pm 0.23$	0	$7.13 \pm 0.33$	$13.2 \pm 3.0$
Sinapic acid (SA)	0	58.93	5.39	0	0	-
CS-SA film	$5.86 \pm 0.38$	$40.49 \pm 0.80$	$7.16 \pm 0.15$	0	$6.94 \pm 0.61$	$12.0 \pm 3.1$
Lignin (LG)	$1.23 \pm 0.08$	$59.1 \pm 0.57$	$6.01 \pm 0.14$	$0.62 \pm 0.33$	$48.16 \pm 2.69$	-
CS-LG film	$5.43 \pm 0.20$	$43.27 \pm 0.15$	$6.32 \pm 0.28$	$0.12 \pm 0.07$	$7.98 \pm 0.29$	$9.7 \pm 5.7$



grafting, the yield of the reaction was quantified for each lignin monomer, based on the elemental analysis of the starting materials and grafted films (Table 1). An increase of the carbon/nitrogen ratio in the grafted polymers was observed compared with the initial chitosan. Considering that nitrogen in the grafted films only derived from chitosan and that additional carbon content in the final polymers was brought by chemical grafting, this allowed the calculation of the reaction yields. The resulting reaction yields were close to 13.8, 13.2 and 12 % for coumaric, ferulic, and sinapic acids, respectively (Table 1). The yield of grafting for each lignin monomer was not very high, although grafting based on carbodiimide ester activation was supposed to be highly efficient in grafting phenolic compounds onto chitosan.<sup>56</sup> However, the grafting reaction may have been greatly affected by the reaction conditions such as chitosan deacetylation degree and molecular weight, initial molar ratio of chitosan/phenolic acids, pH, temperature, and time.<sup>30,57,58</sup>

Furthermore, in this study, ethanol was used as a green solvent for the grafting reaction, but ethanol can also inhibit the reaction by acting as a reactant.<sup>59</sup>

### Grafting of lignin onto chitosan polymer

To further examine the grafting process, the reaction was performed not only with lignin monomers, but also with lignin polymers and evaluated whether this waste product can be valorized without a prior monomer extraction step. UV-Vis, FTIR, and elemental analyses were used as described before to

validate the grafting and to quantify the yield of reaction.

In acetic acid (1 % v/v), lignin showed a characteristic absorbance peak at 280 nm.<sup>60</sup> After reacting with activated lignin, chitosan also exhibited a peak at 280 nm (Figure 6), which indicated successful grafting.

FTIR analysis revealed the presence of lignin on the grafted films (Figure 7). In the FTIR absorbance spectrum of lignin (Figure 7b, brown line), the characteristic peaks of “Sarkanda” lignin could be identified as: 3414  $\text{cm}^{-1}$  ( $\nu_{\text{O-H}}$  of the hydroxyl groups), 2922  $\text{cm}^{-1}$  ( $\nu_{\text{C-H}}$  of the aromatic methoxyl groups), 2851  $\text{cm}^{-1}$  ( $\nu_{\text{C-H}}$  of the methyl- and methylene groups), 1701  $\text{cm}^{-1}$  ( $\nu_{\text{C=O}}$  of the unconjugated carbonyls), 1600  $\text{cm}^{-1}$  and 1515  $\text{cm}^{-1}$  ( $\nu_{\text{C=C}}$  of the aromatic ring and  $\nu_{\text{C=O}}$  of the conjugated carbonyl), 1462  $\text{cm}^{-1}$  ( $\nu_{\text{as C-H}}$ ), 1425  $\text{cm}^{-1}$  ( $\delta_{\text{C-H}}$  of the aromatic ring), 1218  $\text{cm}^{-1}$  ( $\nu_{\text{C=O}}$ ,  $\nu_{\text{C-C}}$  and  $\nu_{\text{C-O}}$ ), 1120  $\text{cm}^{-1}$  ( $\delta_{\text{C-H}}$  of the syringyl units), and 1031  $\text{cm}^{-1}$  ( $\delta_{\text{C-H}}$  of the aromatic ring,  $\nu_{\text{C-O}}$  of the hydroxyl- and ether groups).<sup>61-67</sup> With regard to the FTIR spectrum of lignin grafted onto chitosan (Figure 7a, purple line), it is worthy to note that there was a shift from 1603  $\text{cm}^{-1}$  ( $\delta_{\text{N-H}}$  of amine I) down to 1566  $\text{cm}^{-1}$  ( $\delta_{\text{N-H}}$  of amine II). This shift was related to amine I of deacetylated chitosan monomers, which highlighted a change in the local environment of the reacting amine function (as was previously observed with the lignin monomers). Additional characteristic peaks of lignin also appeared in the spectrum, especially peaks attributed to the aromatic ring vibrations and C-H vibrations of the methoxy groups at 1518  $\text{cm}^{-1}$  and 2846  $\text{cm}^{-1}$ , respectively. The presence of these new absorbance peaks in the final composite polymer unambiguously showed that the lignin had successfully been grafted onto chitosan.

Regarding the monomers, the grafting yield was calculated following the same procedure as described above, which is based on elemental analysis. However, the sulphur content of lignin was used for normalization, because nitrogen was detected both in chitosan and lignin powder (Table 1). The resulting grafting yield was around 9.7 %. It is noteworthy that this yield of grafting was slightly lower than the one obtained for each individual monomer. This could be explained by the steric hindrance of this macromolecule, which could have limited the lignin grafting.

Once the grafting method was proved to be effective, and the yield of the reaction was quantified, it was then important to

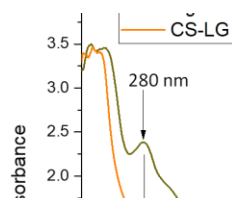


Figure 6: UV-VIS absorbance spectra obtained on the film forming solution after the grafting reaction (followed by dialysis) of lignin onto chitosan (CS: chitosan - LG: lignin). Chitosan and lignin spectra in solution are also displayed for comparison purpose. The arrows point out maximum characteristic absorbance peak.



Wavelength (nm)

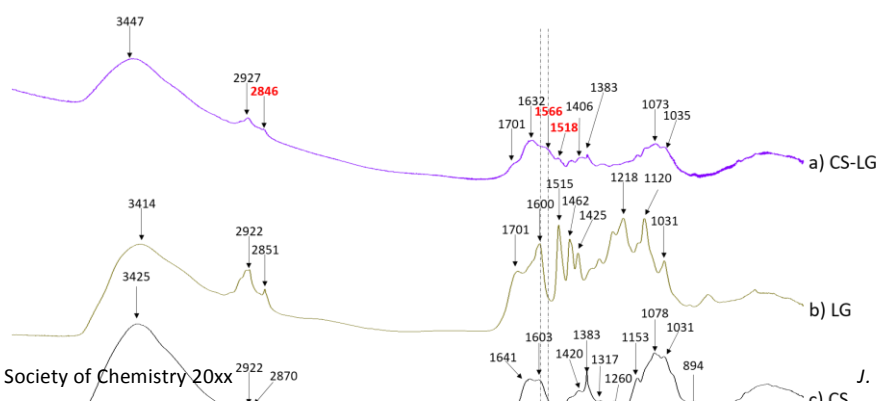


Figure 7: FTIR absorbance spectrum of a) chitosan film grafted with lignin (CS-LG). FTIR spectra of starting materials: b) lignin (LG) and c) chitosan (CS), are also displayed for comparison. The arrows represent the characteristic maximum absorbance peak. Vibrations in red refer to the differences highlighted by FTIR between starting materials and chitosan film grafted with lignin. The dashed lines indicate the shift occurring from 1603  $\text{cm}^{-1}$  ( $\delta_{\text{N-H}}$  of the amine I group) down to around 1560  $\text{cm}^{-1}$  ( $\delta_{\text{N-H}}$  of the amine II group) after the grafting.

evaluate the anti-oxidant properties of the resulting films to consider potential applications of this method to produce active packaging materials.

#### Anti-oxidant activity of lignin and lignin/chitosan grafted films compared to the initial free lignin monomers

The RSA of starting and final grafted materials was evaluated using the DPPH• method.

Figure 8 displays the anti-oxidant properties of acid phenol lignin monomers. Coumaric acid exhibited the lowest RSA (5 % at equilibrium), while ferulic acid displayed an intermediate value (35 %). Among the three lignin monomers, sinapic acid showed a significantly higher RSA, leading to a 70 % decrease of the DPPH• free radicals at equilibrium. This difference in the anti-oxidant activity of lignin monomers could easily be explained by their chemical structure. Lignin monomers are composed of two hydroxyl groups with different degrees of methoxy substitution (Figure 1).

Indeed, coumaric acid has no methoxy groups, whereas ferulic acid is ortho-methoxy substituted, and sinapic acid is di-ortho-methoxy substituted. As reported by Brand-Williams *et al.* (1995), the ortho-methoxy substitution favours the stabilization of the aryloxy radical by electron donation, which therefore increases the radical scavenging activity of the molecule.<sup>31,68</sup> These results, therefore, highlight that the respective ratio of lignin monomers can strongly influence the global anti-oxidant activity of the lignin polymer. In order to obtain stronger anti-radical activity, lignins could be selected based on their constitutive monomers (high sinapic acid and a low coumaric acid content).

The same trend was observed when the monomers were grafted onto chitosan. The chitosan films grafted with coumaric acid displayed almost no anti-oxidant activity (slightly higher than the chitosan films alone), and the one grafted with ferulic acid showed intermediate anti-oxidant activity. Furthermore, sinapic acid grafted films remained the most efficient to scavenge DPPH• free radicals (Figure 9). At equilibrium, the films grafted with coumaric acid led to a decrease of around 9 % of free DPPH• radical, compared with around 50 % for ferulic acid and 90 % for sinapic acid grafted films.

Furthermore, although there was a low grafting yield of lignin onto chitosan, a decrease of around 50 % of the free radical scavenging activity was observed when the lignin was grafted onto chitosan. Based on RSA values obtained for ferulic and

sinapic acid at equilibrium (50 and 90 %, respectively) and on the ferulic/sinapic monomer ratio of "Sarkanda" lignin (about 1.04), a theoretical RSA value of around 70 % at equilibrium can be expected for grafted lignin films. This clearly highlights that the maximum radical scavenging efficiency of grafted lignin films has not been reached. This could be explained by the non-availability of some hydroxyl functions due to steric hindrance or the involvement of reactive groups in the

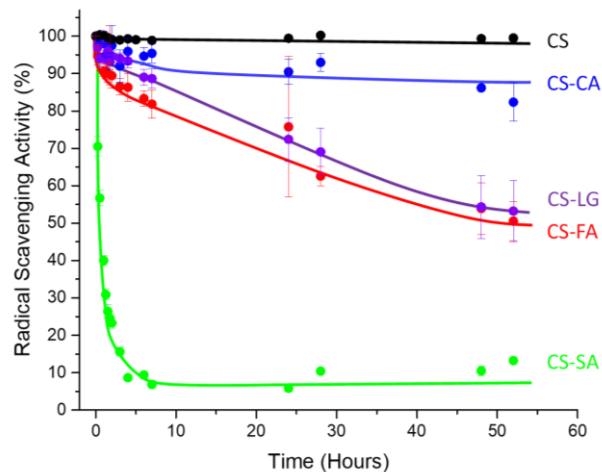


Figure 9: Radical Scavenging Activity of chitosan film (CS) and grafted films with lignin (CS-LG) and lignin monomers (CA: coumaric acid, FA: ferulic acid, SA: sinapic acid) assessed DPPH• test in ethanol (n=3). Lines are eye-guides.

intramolecular bindings of the lignin polymer. This hypothesis was supported by the reaction kinetics of lignin with DPPH•. Indeed, the equilibrium was not fully reached for the films grafted with lignin compared with those grafted with the monomers. However, the diffusion of DPPH• molecules in the film matrix may have been slowed down, and this could explain that the reaction kinetics were decreased compared with lignin monomers grafted films, in which the hydroxyl groups are more easily accessible. Moreover, as grafting occurred with chitosan, there was obviously no migration of active molecules in the solution. Nevertheless, despite a grafting yield of around 10 % and taking into account that reactive groups would not be available, chitosan films grafted with lignin exhibited improved capacity to scavenge free radicals and could be an interesting way to valorize these two industrial waste products and to use them as active materials.

## Conclusions

This study shows that grafting of lignin monomers onto chitosan is feasible, using an intermediate reaction with NHS and EDC as coupling agents, in ethanol as a green solvent. Grafting was detected by UV-Vis absorption, as well as by FTIR spectroscopy, with a shift of the peak attributed to the amine I of chitosan, where the grafting occurred, and with the concomitant appearance of absorbance peaks attributed to the aromatic rings from lignin monomers. In addition, based on carbon, nitrogen and sulphur content, reaction yields of around 13 and 10 % were obtained for lignin monomers and

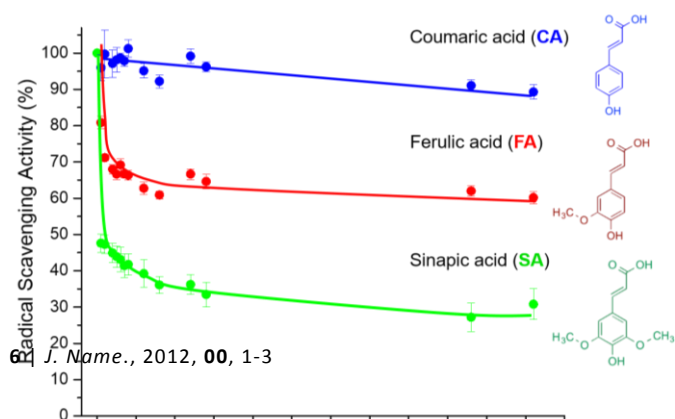


Figure 8: Radical Scavenging Activity of lignin monomers assessed with DPPH• test in ethanol (n=3). Lines are eye-guides.

lignin, respectively. Even if a low reaction yield added anti-oxidant activity to the grafted films, it could be worthwhile to improve the grafting reaction yield.

The anti-oxidant activity of lignin monomers and grafted films was also investigated in this work. Significant differences in the anti-oxidant activity of lignin monomers were noticeable, with a higher radical scavenging activity of sinapic acid due to di-ortho-methoxy substitution. In contrast, coumaric acid displayed no anti-oxidant activity, and ferulic acid had an intermediate activity. Additionally, the anti-oxidant activity of lignin monomers was preserved after grafting onto chitosan, and the respective order of the anti-oxidant activity remained the same. After grafting, the radical scavenging activity occurred without the migration of active substance in the liquid phase in contact.

Furthermore, these results also show that the composition and the ratio of lignin monomers influence the anti-oxidant activity of lignin. Therefore, lignin should be selected based on its constitutive monomers. It will be interesting to determine the anti-oxidant activity of lignin and lignin grafted onto chitosan, which has been extracted from several lignin taxonomies in order to confirm the hypothesis that the higher the syringyl unit concentration is, the higher the anti-oxidant activity becomes. It is also possible to improve the chemical extraction of lignin, and to preferentially select a fraction containing a higher content of sinapic acid and a low content of coumaric acid. This could lead to the identification of the best lignin source, and extraction processing, for the production of active materials, in order to protect sensitive products from oxidation, such as foods or cosmetics, for extending their shelf-life. This first proof of concept sets up the basis to further improve and tune the anti-oxidant activity of the final product.

## Conflicts of interest

There are no conflicts to declare.

## Acknowledgements

This work was supported by the Regional Council of Bourgogne-Franche Comté and The "Fonds Européens de Développement Régional (FEDER). The authors would like to thank Marcel Soustelle for the elemental analysis performed at the technological Platform for Chemical analysis and Molecular synthesis (Institute of the Molecular Chemistry of Burgundy University and Sayens).

## References

- L. Hodasova, M. Jablonsky, A. Skulcova and A. Haz, *Wood Res.*, 2015, **60**, 973-986.
- H. Li and L. Peng, *J. Carbohydr. Polym.*, 2015, **124**, 35-42.
- L. Liu, M. Qian, P. Song, G. Huang, Y. Yu and S. Fu, *Sustain. Chem. Eng.*, 2016, **4**, 2422-2431.
- L. Wei and A. McDonald, *Materials*, 2016, **9**, 303-326.
- F. G. Calvo-Flores and J. A. Dobado, *ChemSusChem*, 2010, **3**, 1227-1235.
- R. C. Pettersen, *The chemistry of solid wood*, 1984, **207**, 57-126.
- F. Rosillo-Calle, P. Groot, S. de Hemstock and J. Woods, *The biomass assessment Handbook: Bioenergy for a sustainable environment*, 2007, 110-143.
- S. Notlev and M. Norgren, *Langmuir*, 2010, **26**, 5484-5490.
- M. Cannatelli and A. Ragauskas, *Appl. Microbiol. Biotechnol.*, 2016, **100**, 8685-8691.
- W. El-Zawawy, M. Ibrahim, M. Belgacem and A. Dufresne, *Mater. Chem Phys.*, 2011, **131**, 348-357.
- S. Laurichesse and L. Avérous, *Prog. Polym. Sci.*, 2014, **39**, 1266-1290.
- A. Singh, K. Yadav and A. Sen, *Am. J. Polym. Sci.*, 2012, **2**, 14-18.
- K. Crouvisier Urion, P. Bodart, P. Winckler, J. Raya, R. Gougeon, P. Cayot, S. Domenek, F. Debeaufort and T. Karbowiak, *Sustain. Chem. Eng.*, 2016, **4**, 6371-6381.
- S. Domenek, A. Louaifi, A. Guinault and S. Baumberger, *J. Polym. Environ.*, 2013, **21**, 692-701.
- T. Saito, R. Brown, M. Hunt, D. Pickel, J. Pickel, J. Messman, F. Baker, M. Keller and A. Naskar, *Green Chem.*, 2012, **14**, 3295-3303.
- C. Wang, S. Kelley and R. Venditti, *ChemSusChem*, 2016, **9**, 770-783.
- L. Chen, C. Tang, N. Ning, C. Wang, Q. Fu and Q. Zhang, *Chinese J. Polym. Sci.*, 2009, **27**, 739-746.
- K. Crouvisier Urion, A. Lagorce-Tachon, C. Lauquin, P. Winckler, W. Tongdeesoontorn, S. Domenek, F. Debeaufort and T. Karbowiak, *Food Chem.*, 2017, **236**, 120-126.
- H. Luo, Q. Shen, F. Ye, Y.-F. Cheng, M. Mezgebe and R.-J. Qin, *Mater. Sci. Eng. C*, 2012, **32**, 2001-2006.
- Y. Pan, J. Zhan, H. Pan, W. Wang, G. Tang, L. Song and Y. Hu, *Sustain. Chem. Eng.*, 2016, **4**, 1431-1438.
- A. Hambardzumyan, M. Molinari, N. Dumelie, L. Foulon, A. Habrant, B. Chabbert and V. Aguié-Béghin, *Comptes Rendu Biol.*, 2011, **334**, 839-850.
- S. Wang, Y. Sun, F. Kong, G. Yang and P. Fatehi, *Bioresource*, 2016, **11**, 1765-1783.
- S. Wang, Z. Zhou, H. Xiang, W. Chen, Y. Erqiang, T. Chang and M. Zhu, *Compos. Sci. Technol.*, 2016, **128**, 116-122.
- R. Shi and B. Li, *Starch J.*, 2016, **68**, 1224-1232.
- P. Chen, L. Zhang, S. Peng and B. Liao, *J Appl Polym. Sci.*, 2006, **101**, 334-341.
- Y. Jeon, J. Kamil and F. Shahidi, *J. Agric. Food Chem.*, 2002, **50**, 5167-5178.
- C. Nunes, M. A. Coimbra and P. Ferreira, *Chem. Record*, 2018, **18**, 1-13.
- A. Hambardzumyan, L. Foulon, B. Chabbert and V. Aguié-Béghin, *Biomacromolecules*, 2012, **13**, 4081-4088.
- C. Madeleine-Perdrillat, T. Karbowiak, J. Raya, R. Gougeon, P. Bodart and F. Debeaufort, *Carbohydr. Polym.*, 2015, **118**, 107-117.
- S. Woranuch and R. Yoksan, *Carbohydr. Polym.*, 2013, **96**, 495-502.
- W. Brand-Williams, M. Cuvelier and C. Berset, *LWT Food Sci. Technol.*, 1995, **28**, 25-30.
- C. Popovici, I. Saykova and B. Tylkowski, *R. Génie Indus.*, 2009, **4**, 25-39.
- C. Park, C. Vo, T. Kang, E. Oh and B. Lee, *Eur. J. Pharm. Biopharm.*, 2015, **89**, 365-373.
- M. A. Z. Farag, AH, M. Hamed, Z. Kandeel, H. El-Rafie and R. El-Akad, *Nat. Prod. Res.*, 2015, **29**, 116-124.
- G. Pan, C. Thompson and G. Leary, *J Wood Chem. Technol.*, 2002, **22**, 137-146.
- J. Liu, J. Lu, J. Kan and C. Jin, *Int. J. Biol. Macromol.*, 2013, **62**, 321-329.
- M. Xie, B. Hu, Y. Wang and X. Zeng, *J. Agric. Food Chem.*, 2014, **62**, 9128-9136.



- 38 O. Abbas, G. Compère, Y. Larondelle, D. Pompeu, H. Rogez and V. Baeten, *Vib. Spectrosc.*, 2017, **92**, 111-118.
- 39 R. Clavijo, D. Ross and R. Aroca, *J. Raman Spectrosc.*, 2009, **40**, 1984-1988.
- 40 M. Kowczyk-Sadowy, R. Swislocka, H. Lewandoska, J. Piekut and W. Lewandoski, *Molecules*, 2015, **20**, 3146-3169.
- 41 R. Swislocka, M. Kowczyk-Sadowy, M. Kalinowska and W. Lewandoski, *Spectrosc.*, 2012, **27**, 35-48.
- 42 J. M. Dimitric-Markovic, U. B. Mioc, J. M. Baranac and Z. P. Nedic, *J. Serbian Chem. Soc.*, 2001, **66**, 451-462.
- 43 E. Ferrer, M. Salinas, M. Correa, F. Vrdoljak and P. Williams, *Zeitschrift für Naturforschung B*, 2005, **60**, 305-311.
- 44 M. Kalinowska, J. Piekut, A. Bruss, C. Follet, J. Sienkiewicz-Gromiuk, R. Swislocka, Z. Rzaczyńska and W. Lewandoski, *Spectrochim. Acta A*, 2014, **122**, 631-638.
- 45 N. Kumar and V. Pruthi, *Biotechnol.*, 2015, **5**, 541-551.
- 46 R. Panwar, A. K. Sharma, M. Kaloti, D. Dutt and V. Pruthi, *Appl. Nano.*, 2016, **6**, 803-813.
- 47 S. E. Sajjadi, Y. Shokoohinia and N. S. Moayedi, *Jundishapur J. Nat. Pharm. Prod.*, 2012, **7**, 159-162.
- 48 M. Belkov, S. Brinkevich, S. Samovich, I. Skorniyakov, G. Tolstorozhev and O. Shadyro, *J. Appl. Spectrosc.*, 2012, **78**, 794-801.
- 49 K. Rasheeda, H. Bharathy and N. Nishad Fathima, *Int. J. Biol. Macromol.*, 2018, **113**, 952-960.
- 50 R. Swislocka, *Spectrochim. Acta A*, 2013, **111**, 290-298.
- 51 M. Fernandes Queiros, K. R. T. Melo, D. A. Sabry, G. L. Sasaki and H. A. O. Rocha, *Mar. Drugs*, 2015, **13**, 141-158.
- 52 J. Kumirska, M. Czerwicka, Z. Kaczynski, A. Bychowska, K. Brzozowski, J. Thöming and P. Stepnowski, *Mar. Drugs*, 2010, **8**, 1567-1636.
- 53 J. Liu, X. Wen, J. Lu and C. Jin, *Int. J. Biol. Macromol.*, 2014, **65**, 97-106.
- 54 P. Negrea, A. Caunii, I. Sarac and M. Butnariu, *Digest J. Nano. Biostruct.*, 2015, **10**, 1129-1138.
- 55 S. M. Silva, C. R. Braga, M. V. Fook, C. M. Raposo, L. H. Carvalho and E. L. Canedo, *Materials Science, Engineering and Technology*, 2012, 43-63.
- 56 J. Liu, P. Huimin, S. Liu, J. Kan and C. Jin, *Carbohydr. Polym.*, 2017, **174**, 999-1017.
- 57 A. O. Aytakin, S. Morimura and K. Kida, *J. Biosci. Bioeng.*, 2011, **111**, 212-216.
- 58 S. B. Schreiber, J. J. Bozell, D. G. Hayes and S. Zivanovic, *Food Hydrocoll.*, 2013, **33**, 207-214.
- 59 P. Guo, J. D. Anderson, J. J. Bozell and S. Zivanovic, *Carbohydr. Polym.*, 2016, **140**, 171-180.
- 60 M. Jablonsky, J. Kocis, A. Haz and J. Sima, *Cell. Chem. Technol.*, 2015, **49**, 267-274.
- 61 E. C. Achinivu, *Int. J. Mol. Sci.*, 2018, **19**, 428-442.
- 62 C. A. Borges Cateto, Thesis, Grenoble Alpes University, 2008.
- 63 O. Derkacheva and D. Sukhov, *Macromolecular Symp.*, 2008, **265**, 61-68.
- 64 N.-E. El Mansouri, Q. Yuan and F. Huang, *Bioresour.*, 2011, **6**, 2647-2662.
- 65 L. M. Kline, D. G. Hayes, A. R. Womac and N. Labbé, *Bioresour.*, 2010, **5**, 1366-1383.
- 66 T. Yan, Y. Xu and C. Yu, *J Appl Polym. Sci.*, 2009, **1141**, 1896-1901.
- 67 G. Zhou, G. Taylor and A. Polle, *Plant Methods*, 2011, **7**.
- 68 F. Shahidi and P. Ambigaipalan, *J. Funct. Food.*, 2015, **18**, 820-897.
- 69 H.-L. Li, D. She, Paipeng, Q. Xu, J.-K. Liu, X.-M. Zhang and Z. Chaogeng, *Cell. Chem. Technol.*, 2017, **51**, 433-445.